Multiplet structure of the defect modes in 1D helical photonic crystals with twist defects

2005 J. Phys. A: Math. Gen. 38 8821

(http://iopscience.iop.org/0305-4470/38/41/001)

INSTITUTE OF PHYSICS PUBLISHING JOURNAL OF PHYSICS A: MATHEMATICAL AND GENERAL

J. Phys. A: Math. Gen. **38** (2005) 8821–8840 doi:10.1088/0305-4470/38/41/001

Multiplet structure of the defect modes in 1D helical photonic crystals with twist defects

C G Avendaño[1], S Ponti[2], J A Reyes[1] and C Oldano[2]

[1] Instituto de Física, Universidad Nacional Autónoma de México, Apdo. P 20-364 01000, México DF, Mexico
[2] Dipartimento di Fisica Politecnico di Torino and INFM, Corso Duca degli Abruzzi 24, 10129 Torino, Italy

Received 18 May 2005, in final form 30 August 2005
Published 28 September 2005
Online at stacks.iop.org/JPhysA/38/8821

Abstract

We theoretically analyse the defect modes generated by equispaced twist defects in 1D helical (cholesteric-like) structures within their frequency gap which is such that only the first two of the four eigenwaves $1^{\pm}, 2^{\pm}$ are exponentially attenuated. n_0 identical defects generate n_0 different defect modes, each one represented by a linear combination of the four eigenwaves. The components 1^{+} and 1^{-} are by far the dominant ones and they are localized near the defect planes. We give exact analytic expressions for the elements of the transfer and scattering matrices of the defect planes, for the functions defining the defect mode when $n_0 = 1$, and for the defect frequencies when $n_0 = 1, 2, 3$. In the particular case $n_0 = 2$ and twist angle $\theta = \pi/2$, the difference between the two defect wavelengths $\lambda_{d2}, \lambda_{d1}$ depends exponentially on the distance z_1 between the defect planes, going to zero for $z_1 \to \infty$ and becoming as large as the entire frequency gap for $z_1 \to 0$.

PACS numbers: 42.70.Qs, 42.70.Df

1. Introduction

One or more defects in a periodic structure may give rise to resonant modes inside the photonic band gaps, namely to standing waves with a huge energy density localized in the proximity of the defects (*defect modes*). A conventional 1D structure with only one defect can be considered as a Fabry–Perot interferometer in which the reflecting layers at the two sides of the cavity are constituted by 1D crystals whose thickness is comparable with the attenuation length of the standing waves within the gap, which are exponentially attenuated. The cavity acts here as a defect in the periodic structure. Very interesting optical properties are obtained by considering (1) anisotropic periodic structures, which display two different sets of band gaps for light with different polarization states, and (2) samples with more than one defect.

In this paper, we theoretically consider light propagation along the helix axis of samples in which the periodic structures are helical (cholesteric-like) crystals and the thickness of the

cavities goes to zero. Any defect reduces therefore to a simple discontinuity plane within the periodic structure. Such samples can be obtained as follows: (1) we consider first an helical sample without defects between planes orthogonal to the helix axis; (2) then we cut the sample in such a way to obtain two or more layers between parallel planes; and (3) we finally rotate any layer with respect to the preceding one around their common helix axis by a given angle (*twist angle*). Samples with only one twist defect in the middle have received a great deal of attention in recent years because of their interesting optical [1–8] and acoustical [9–11] properties and for applications [12–14]. Helical media without defects are unique periodic structures of great practical interest whose optical properties can be defined by equations which, for light propagating along the helix axis (parallel propagation), are at the same time exact and very simple. The four eigenwaves are obviously Bloch waves, but with a suitable choice of reference frame they can be written in the simple form of plane waves with constant wavevectors. Such vectors satisfy the same dispersion relation valid for *homogeneous* anisotropic media, that is, a biquadratic equation. As far as we know, nothing similar is found for any other periodic medium. In fact, the Bloch waves are the superposition of an infinite number of plane waves even in the simple case of periodically spaced isotropic layers [15]. Since the defect modes in periodic media with defects are the superposition of Bloch waves their description requires, in general, the use of complicated equations or computations, with the only exceptions of helical structures with twist defects. This fact is in itself a good reason for their study, in our opinion. Some interesting results have already been found recently for samples with only one twist defect [2, 3, 6, 7]. This paper can be considered as a continuation of the already published ones, with the extension to samples with any number of twist defects. The considered cholesteric-like structure is, at the same time, dielectric and magnetic. At the optical frequencies, the relative permeability of any medium is practically equal to one, but our results are valid for any frequency. The addition of a permeability tensor μ to the permittivity tensor ε gives equations which are both more general and simple, at least in the sense that they are more symmetric. Further, a suitable choice of the permittivity and permeability tensors greatly simplifies the equations.

In section 2, we define the optical properties of the helical structure without defects which are strictly required for the analysis of the twist defects. Most such properties are already known and have been described in innumerable papers and textbooks. In particular, exact analytic solutions for parallel propagation in cholesteric liquid crystals have been known since 1971 [16]. The central part of this section concerns the properties of the standing waves within the band gap (section 2.3). In section 3, we discuss the optical properties of samples with only one twist defect, giving for the first time exact equations for the defect mode and for the transfer and scattering matrices of the defect plane. Samples with two or more twist defects are discussed in sections 4 and 5, respectively. Finally, in section 6 we give our final comments and concluding remarks.

2. Optical properties of the helical structure

We consider a dielectric and magnetic medium in which the tensors defining the local permittivity $\varepsilon\varepsilon_0$ and permeability $\mu\mu_0$ rotate uniformly along a given axis, say x_3, with their principal axes making constant angles with x_3 (helically 1D-periodic medium).

2.1. The propagation equation and its solutions

For parallel propagation the Maxwell equations can be written as

$$\frac{\mathrm{d}\beta}{\mathrm{d}z} = \mathrm{i}H\beta, \tag{1}$$

where

$$z = \frac{\omega}{c} x_3, \tag{2}$$

$$\beta = \begin{pmatrix} e_1 \\ e_2 \\ h_1 \\ h_2 \end{pmatrix} = \mathcal{R}(-qz) \begin{pmatrix} Z_0^{-1/2} E_1 \\ Z_0^{-1/2} E_2 \\ Z_0^{1/2} H_1 \\ Z_0^{1/2} H_2 \end{pmatrix} \qquad H = \begin{pmatrix} 0 & -\mathrm{i}\widetilde{\lambda} & 0 & \mu_2 \\ \mathrm{i}\widetilde{\lambda} & 0 & -\mu_1 & 0 \\ 0 & -\varepsilon_2 & 0 & -\mathrm{i}\widetilde{\lambda} \\ \varepsilon_1 & 0 & \mathrm{i}\widetilde{\lambda} & 0 \end{pmatrix}, \tag{3}$$

and where $Z_0 = \sqrt{\mu_0/\varepsilon_0}$; E_i, H_i, $(i = 1, 2)$ are the transversal components of the field vectors $\mathbf{E}$, $\mathbf{H}$; $\mathcal{R}(\varphi)$ is the rotation matrix defined as

$$\mathcal{R}(\varphi) = \exp(\mathrm{R}\varphi) \equiv \cos\varphi\, \mathbf{I} + \sin\varphi \mathrm{R}, \qquad \mathrm{R} = \begin{pmatrix} 0 & -1 & 0 & 0 \\ 1 & 0 & 0 & 0 \\ 0 & 0 & 0 & -1 \\ 0 & 0 & 1 & 0 \end{pmatrix}; \tag{4}$$

$\mathbf{I}$ is the 4×4 identity matrix,

$$\widetilde{\lambda} = \lambda / p, \tag{5}$$

$p = 2\pi/q$ is the helix pitch and λ the wavelength in free space. The helix is right- and left-handed for positive and negative values, respectively, of p and $\widetilde{\lambda}$. In the following, we consider the right-handed helices. The quantities e_i, h_i can be considered as normalized components of the field vectors $\mathbf{E}$, $\mathbf{H}$ in a Cartesian frame (x_1, x_2, x_3) whose axes x_1 and x_2 are rotating solidly with the tensors ε, μ. In the rotating frame, these tensors are therefore independent of x_3 and z. The parameters ε_i, μ_i depend on the principal values of ε, μ and on the angles between their principal axes and the Cartesian axes. The simple form (4) of $\mathbf{H}$ is obtained by suitably choosing the rotating axes x_1 and x_2. The structure considered here includes, as particular cases, the chiral smectic-C (S_C^*) and cholesteric (N*) liquid crystals. In such crystals $\mu = 1$, one of the principal axes of ϵ is orthogonal to x_3, another one makes a constant tilt angle with x_3 for S_C^* and is orthogonal to x_3 for N*. In the last case, x_1, x_2 and x_3 are the principal axes and ε_1, ε_2 and ε_3 are the principal values of ε. In the other cases, we must diagonalize the projection of the tensors ε and μ on the plane orthogonal to x_3 in order to define x_k, ε_k, μ_k $(k = 1, 2)$. The evaluation of such quantities is standard.

Since the system matrix H is z-independent, the propagation equation (1) admits four solutions having the form of plane waves

$$\beta^j(z) = t^j \exp(\mathrm{i} n_j z), \tag{6}$$

where the time factor $\exp(-\mathrm{i}\omega t)$ is omitted and where n_j, t^j are the eigenvalues and eigenvectors of H, respectively. They are given by the equations:

$$n_{1,2}^2 = \frac{\varepsilon_1\mu_2 + \varepsilon_2\mu_1}{2} + \widetilde{\lambda}^2 \mp u \tag{7}$$

$$\begin{aligned} t_1^{\pm} &= c_1(\pm n_1 u_1, \mathrm{i}\widetilde{\lambda}(2\varepsilon_1\mu_m - u_2), \mp 2\mathrm{i} n_1 \widetilde{\lambda}\epsilon_m, 2\widetilde{\lambda}^2\epsilon_m + u_1\epsilon_1) \\ t_2^{\pm} &= c_2(\pm n_2 u_2, \mathrm{i}\widetilde{\lambda}(2\varepsilon_1\mu_m - u_1), \mp 2\mathrm{i} n_2 \widetilde{\lambda}\epsilon_m, 2\widetilde{\lambda}^2\epsilon_m + u_2\epsilon_1), \end{aligned} \tag{8}$$

where

$$\begin{aligned} &u = \sqrt{4\varepsilon_m\mu_m\widetilde{\lambda}^2 + a_\mathrm{c}^2}, && u_{1,2} = a_\mathrm{c} \mp u, \\ &c_k = |4n_k u(u_k\varepsilon_1 + 2\widetilde{\lambda}^2\varepsilon_m)|^{-1/2}, && (k = 1, 2) \\ &a_\mathrm{c} = \frac{\varepsilon_1\mu_2 - \varepsilon_2\mu_1}{2}, && \varepsilon_m = \frac{\varepsilon_1 + \varepsilon_2}{2}, \qquad \mu_m = \frac{\mu_1 + \mu_2}{2}. \end{aligned} \tag{9}$$

2.2. Amplitude representation and metric of the state space

The internal field can be represented as a superposition of the four eigenwaves (*amplitude representation*), by setting

$$\beta(z) = a_j t^j \exp(\mathrm{i}n_j z) \equiv T\alpha(z) \tag{10}$$

where T is the matrix whose jth column coincides with t^j and $\alpha(z)$ is the 4-vector with components $a_j \exp(\mathrm{i}n_j z)$. Obviously, α and $\beta = T\alpha$ represent the same state in two different sets of basis vectors. The metric of the state space is obtained by defining a metric tensor G and a scalar product $\beta_1^\dagger G_\beta \beta_2 \equiv \alpha_1^\dagger G_\alpha \alpha_2$, where G_β and $G_\alpha = T^\dagger G_\beta T$ are the matrices representing G in the two sets of basis vectors. Setting

$$G_\beta = \begin{pmatrix} 0 & 0 & 0 & 1 \\ 0 & 0 & -1 & 0 \\ 0 & -1 & 0 & 0 \\ 1 & 0 & 0 & 0 \end{pmatrix} \tag{11}$$

the norm of the state vector represents the time average of the z-component of the Poynting vector, and the tensor G satisfies the relations

$$G \equiv G^\dagger \equiv G^{-1}. \tag{12}$$

In lossless media, the z-derivative of the norm is identically zero and the matrix $G_\beta H$ is self-adjoint:

$$G_\beta H = (G_\beta H)^\dagger \equiv H^\dagger G_\beta. \tag{13}$$

The above property and the fact that the eigenvalue equation for H is biquadratic imply that the eigenvalues are $n_1, n_2, n_3 = -n_1, n_4 = -n_2$, with n_j real or purely imaginary.

2.3. Properties of the standing waves within the band gap

The helical structure considered here admits only one band gap, where n_1 is imaginary and n_2 real. At the band edges 1 and 2, the eigenvalue n_1 is equal to zero, the reduced wavelengths $\widetilde{\lambda}_k$ ($k = 1, 2$) are given by $\sqrt{\varepsilon_k \mu_k}$, and the corresponding eigenvectors $1^\pm$ define linearly polarized standing waves whose amplitudes exponentially decrease in the forward direction[3]. Interestingly, the field vectors **e** and **h** are parallel and oscillate along the axis x_k with a phase difference $\Delta\varphi = \pm\pi/2$. In fact equation (8) gives eigenwaves $1^\pm$ with $\mathbf{h}^\pm$ real and $\mathbf{e}^\pm$ purely imaginary. In the particular case $a_c = 0$ the vector $\mathbf{e}^+$ is parallel to $\mathbf{h}^+$ and $\mathbf{e}^-$ to $\mathbf{h}^-$ for any $\widetilde{\lambda}$ within the gap. The angles between such vectors and the axis x_2 are $\pm\phi$, where

$$\widetilde{\lambda} = \widetilde{\lambda}_m + \widetilde{\lambda}_a \cos 2\phi, \tag{14}$$

with

$$\widetilde{\lambda}_m = \frac{\widetilde{\lambda}_1 + \widetilde{\lambda}_2}{2}, \qquad \widetilde{\lambda}_a = \frac{\widetilde{\lambda}_2 - \widetilde{\lambda}_1}{2}. \tag{15}$$

Therefore, the field vectors of the eigenwaves 1^+ and 1^- rotate by $\pi/2$ in opposite senses when $\widetilde{\lambda}$ increases from $\widetilde{\lambda}_1$ to $\widetilde{\lambda}_2$ (without loss of generality we assume $\widetilde{\lambda}_1 < \widetilde{\lambda}_2$). The sense of their rotation satisfies the right-hand rule with respect to the forward direction of the two eigenwaves.

[3] Here 'forward' does not refer to the direction of the energy flow since the Poynting vector is zero. The waves 1^+ and 1^- must be considered forward and backward respectively, even though they are standing, because a wave incident on a discontinuity plane from the left (a 'forward' wave) generates 1^+ in transmission and 1^- in reflection.

In the general case, $a_c \neq 0$ the vectors **e** and **h** are no more parallel during the rotation but their bisector $\phi \equiv (\phi_e + \phi_h)/2$ makes angles with x_2 which are still approximately given by equation (14). The angle ψ between **e** and **h** plays a main role for the optical properties of the defect modes. Its dependence on a_c and $\widetilde{\lambda}$ is discussed in [2].

We finally observe that within the gap the polarization of the propagating eigenwaves $2^{\pm}$ is nearly circular.

2.4. Metric matrices

In the α-representation, the basis vectors will be chosen in the order 1^+, 2^+, 1^- and 2^-. Using this choice the matrix G_α is given by

$$\begin{pmatrix} 1 & 0 & 0 & 0 \\ 0 & 1 & 0 & 0 \\ 0 & 0 & -1 & 0 \\ 0 & 0 & 0 & -1 \end{pmatrix} \quad \text{and} \quad \begin{pmatrix} 0 & 0 & -\mathrm{i} & 0 \\ 0 & 1 & 0 & 0 \\ \mathrm{i} & 0 & 0 & 0 \\ 0 & 0 & 0 & -1 \end{pmatrix}, \tag{16}$$

in the regions outside and within the band gap, respectively. These matrices summarize the most important properties of the scalar product between the eigenvectors of H. One may note that the norm of the standing waves $1^{\pm}$ within the gap is equal to zero. Another way to define the scalar product consists in assuming as G_β the diagonal matrix with diagonal elements ε_1, ε_2, μ_1 and μ_2. With such definition, the norm of the state vector represents the time average of the energy density[4] multiplied by the velocity of light in free space. It is therefore positive definite, but the simple form of equations (16) is lost since the matrix G_α is no longer sparse.

3. Singlets

We consider now a helical sample between the planes $z = -\ell$ and $z = +\ell$ with only one twist defect at $z = 0$, which divides the sample in two regions referred as a for $z < 0$ and b for $z > 0$. The main properties of the defect mode have already been found numerically in [2, 6, 7, 12]. We approach here the problem quantitatively by means of exact equations.

3.1. Thick Samples

Let us first consider an unbounded structure, i.e., the limit $l \to \infty$. Any solution of Maxwell's equations can be written as

$$\beta(z) = \beta_{\mathrm{a}}(z)\Theta(z) + \beta_{\mathrm{b}}(z)\Theta(-z), \tag{17}$$

where $\Theta(z)$ is the Heaviside step function and $\beta_k(z)$ $(k = a, b)$ is a linear combination of the eigenwaves $t_k^j \exp(\mathrm{i}n_j z)$. The eigenvectors t_{a}^j and t_{b}^j are given by equation (8) in two different frames a and b whose axes $x_{2\mathrm{a}}$, $x_{2\mathrm{b}}$ make an angle θ (see figure 1 in section 3.2). In a frame having as axis x_2 the bisector of $x_{2\mathrm{a}}$, $x_{2\mathrm{b}}$, such vectors are obtained by applying the rotation matrices $\mathcal{R}(-\theta/2)$ and $\mathcal{R}(\theta/2)$ to the vectors t^j defined by equation (8). The corresponding matrices T_{a} and T_{b} are therefore given by

$$T_{\mathrm{a}} = \mathcal{R}(-\phi)T, \qquad T_{\mathrm{b}} = \mathcal{R}(\phi)T, \tag{18}$$

where $\phi = \theta/2$.

[4] We neglect here dispersion. For the definition of the energy density in dispersive media see, e.g., [17].

In the limit $\ell \to \infty$ the exponential factors of the first component of $\alpha_a = T_a^{-1}\beta_a$ and of the third component of $\alpha_b = T_b^{-1}\beta_b$ (corresponding to the eigenwaves 1^+ in the region a and 1^- in the region b) diverge for z going to $-\infty$ and $+\infty$, respectively. Their amplitude must therefore be zero. The tangential continuity of the vectors $\mathbf{E}$ and $\mathbf{H}$ at $z = 0$ give four homogeneous equations for the other six components. Without loss of generality, we can set to 1 the amplitude of the eigenwave 1^- at $z = 0^-$. The amplitudes of the eigenwaves $2^\pm$ at $z = 0^-$ and $z = 0^+$ can easily be expressed as a function of the amplitude s of the eigenwave 1^+ at $z = 0^+$, and the most general internal field can be written as a linear combination of the solutions corresponding to $s = \pm 1$. For each one of such values, the amplitude vectors $\alpha_a(s)$ and $\alpha_b(s)$ have components $(0, A^+(s), 1, A^-(s))$ and $(s, B^+(s), 0, B^-(s))$, respectively, where

$$A^\pm(s) = a'(s) \pm \mathrm{i}a''(s), \qquad B_b^\pm(s) = sA_a^\mp(s), \tag{19}$$

with

$$\begin{aligned} a'(s) &= -\frac{c_2}{a_c c_1}\frac{2\widetilde{\lambda}^2\varepsilon_m + \varepsilon_1 u_1}{2\widetilde{\lambda}^2\varepsilon_m + \varepsilon_1 u_2}\left[\frac{\mathrm{i}n_1\widetilde{\lambda}u\varepsilon_m(\cot\phi)^s s}{2\widetilde{\lambda}^2\varepsilon_m + \varepsilon_1 u_1} + \frac{u_2}{2}\right] \\ a''(s) &= \frac{c_2}{a_c c_1}\frac{2\widetilde{\lambda}^2\varepsilon_m + \varepsilon_1 u_1}{4\widetilde{\lambda}\varepsilon_m n_2}\left[u(\tan\phi)^s s - \frac{2\mathrm{i}n_1\widetilde{\lambda}\varepsilon_m u_1}{2\widetilde{\lambda}^2\varepsilon_m + \varepsilon_1 u_1}\right]. \end{aligned} \tag{20}$$

At each side of the defect plane the amplitudes $A^\pm$ and $B^\pm$ have the same modulus $m = \sqrt{a'^2 + a''^2}$. Therefore, their superposition is a standing wave. It is linearly polarized and *nonlocalized*, whereas the eigenwaves $1^\pm$ define a *localized* standing wave in which the amplitude of the field vectors depends on z as $\exp(-|z|/\ell_d)$, where

$$\ell_d = 1/|n_1| \tag{21}$$

is the attenuation length.

For $s = 1$ the ratio $\rho(\widetilde{\lambda}) = 1/2m^2$ between the square amplitudes of the localized and nonlocalized components at the defect plane depends strongly on $\widetilde{\lambda}$ and reaches an enhanced maximum at a well-defined value $\widetilde{\lambda}_d$ of $\widetilde{\lambda}$. It defines therefore a *quasilocalized* defect mode having the structure of a singlet in which the localized components 1^- and 1^+ are dominant. The fact that the defect mode in helical media with a twist defect is not a *localized mode* in the strict sense, since it also contains a small nonlocalized component, was shown first in [10] for the acoustic waves and extended to the electromagnetic waves in [2, 7, 12]. Some doubts are expressed in [8] about the existence of a nonlocalized component because there is no evidence of this component in region b when the defect mode is excited by waves incident from the left on thick samples. The absence of such component will be explained in the next section. Here we add some comments concerning the use of the found solutions.

(i) It is always possible to find a linear combination of the two solutions in which the eigenwave 2^- is absent in b and 2^+ has unit amplitude in a (at $z = 0^-$). Since this last eigenwave is the only one incident on the defect plane, the amplitudes of the other four eigenwaves coincide with four of the 16 elements of the scattering matrix S of the defect plane. In section 3.2, the defect frequency will be defined using this property. In section 3.3, the scattering matrix will be defined with a different approach.

(ii) The solutions found here define two of the four eigenmodes for the electromagnetic field in finite samples. The other two can be found by considering also the eigenwaves which have been neglected (1^+ in a and 1^- in b). In thick samples (with $l \gg l_d$), we can chose such eigenwaves as independent eigenmodes. They are different from zero only near the boundaries of the sample (boundary eigenmodes). In thin samples, such eigenwaves are not eigenmodes since it is impossible to satisfy the continuity equations at the defect plane without considering also the other eigenwaves.

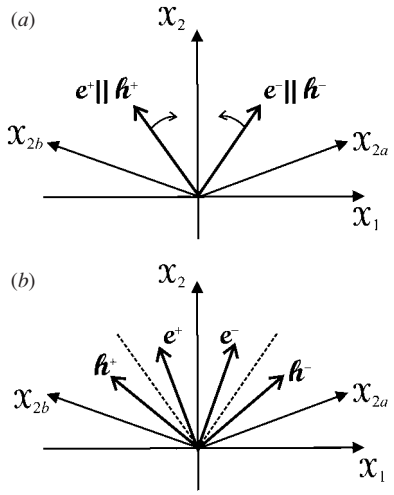

Figure 1. Rotation of the vectors $(\mathbf{e}^+, \mathbf{h}^+)$ and $(\mathbf{e}^-, \mathbf{h}^-)$ of the eigenwaves 1^+ and 1^- for $a_c = 0$ (a) and $a_c \neq 0$ (b). The vectors $(\mathbf{e}^-, \mathbf{h}^-)$ are along x_{2a} and $(\mathbf{e}^+, \mathbf{h}^+)$ along x_{2b} for $\widetilde{\lambda} = \widetilde{\lambda}_2$. By decreasing $\widetilde{\lambda}$ they rotate towards x_2 keeping their parallelism only when $a_c = 0$. For $\widetilde{\lambda} = \widetilde{\lambda}_d$ the vectors $(\mathbf{e}^-, \mathbf{h}^-)$ coincide with $(\mathbf{e}^+, \mathbf{h}^+)$ and along x_2 in (a). In (b) such vectors never coincide but for $\widetilde{\lambda} = \widetilde{\lambda}_d$ their bisectors become parallel to x_2. We recall that the angle between x_{2a} and x_{2b} is the twist angle θ.

(iii) The internal field generated by external waves is the superposition of the four eigenmodes, which in thick samples have the simple structure defined in (ii).

3.2. Wavelength $\widetilde{\lambda}_d$ of the defect mode

In [6], the author shows that the defect wavelength $\widetilde{\lambda}_d$ is approximately given by the equation:

$$\widetilde{\lambda}_d = \widetilde{\lambda}_m + \widetilde{\lambda}_a \cos\theta. \tag{22}$$

We show here that this equation is exact when $a_c = 0$. In this particular case, it is possible to satisfy the continuity relations for **e** and **h** by considering only the eigenwave 1^- in a and 1^+ in b. The possibility of satisfying four relations with only two free parameters is due to the fact that the continuity of **e** implies the continuity of **h** (we recall that such vectors are parallel when $a_c = 0$). Figure 1(a) shows that $\mathbf{e}^+$ and $\mathbf{e}^-$ coincide when they are parallel to the axis x_2, which is the bisector of the twist angle θ. This occurs at a well-defined value $\widetilde{\lambda}_c$ of $\widetilde{\lambda}$, which is related to the angle $\phi = \theta/2$ by equation (14). Therefore, equation (22) defines the exact value of the defect frequency. In conclusion, the defect mode is localized in the strict sense and its frequency is perfectly defined when $a_c = 0$.

Figure 1(b) illustrates the fact that for $a_c \neq 0$ the vectors **e** and **h** are no more parallel during their rotation. It corresponds to $s = 1$ (for $s = -1$ the vectors $\mathbf{e}^-, \mathbf{h}^-$ are unchanged whereas $\mathbf{e}^+, \mathbf{h}^+$ have the opposite directions). Obviously, no value of $\widetilde{\lambda}$ exists for which $\mathbf{e}^+$ coincide with $\mathbf{e}^-$ and $\mathbf{h}^+$ with $\mathbf{h}^-$. The solution found in section 3.1 is obtained by adding to the eigenwaves $1^\pm$ a linear combination of the eigenwaves $2^\pm$, which is such that the resulting vectors **e** and **h** are again parallel, along x_2, and dephased by $\pm\pi/2$ (for $s = -1$ they are parallel to x_1). The figure suggests also that the minimum value of the coefficients $A^\pm$ and $B^\pm$ is obtained when the bisectors of the vectors $(\mathbf{e}^+, \mathbf{h}^+)$ and $(\mathbf{e}^-, \mathbf{h}^-)$ (dotted lines) coincide with x_2, thus giving a maximum for the function $\rho(\widetilde{\lambda})$. Approximate values for $\widetilde{\lambda}_d$ and for $\rho(\widetilde{\lambda})$ have been obtained in [2] on the basis of similar arguments.

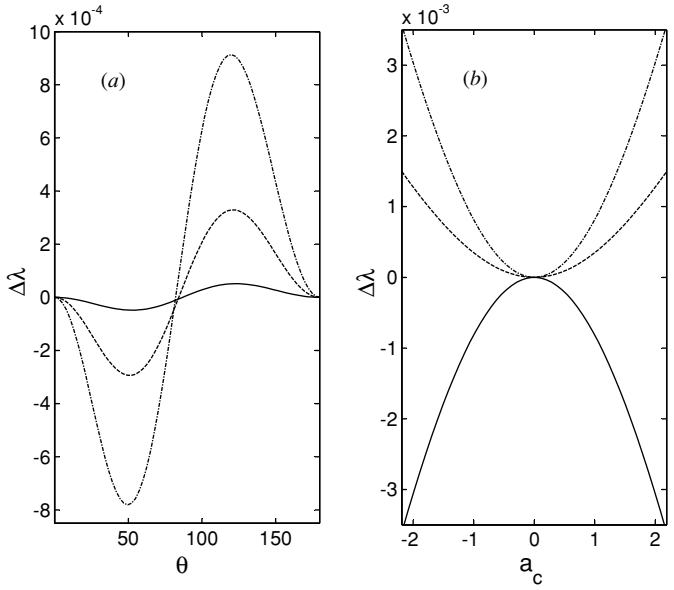

Figure 2. Difference $\Delta\widetilde{\lambda}$ between the exact values of $\widetilde{\lambda}_{\mathrm{d}}$ and the approximate ones (given by equation (22)) versus the twist angle θ in (*a*) and versus the anisotropy parameter a_{c} in (*b*). In (*a*) the full, dashed and dash-dotted lines correspond to $\varepsilon_2 = 2.5, 3, 3.5$, respectively, for $\varepsilon_1 = 2, \mu_1 = \mu_2 = 1$. In (*b*) they correspond to $\theta = \pi/4, 2\pi/4, 3\pi/4$, with $\widetilde{\lambda}_1 \equiv \sqrt{\varepsilon_1\mu_1} = 1.7, \widetilde{\lambda}_2 \equiv \sqrt{\varepsilon_2\mu_2} = 2.3$, and $Z_m = 0.67$, where $Z_m \equiv 1/2(\sqrt{\mu_2/\varepsilon_2} - \sqrt{\mu_1/\varepsilon_1})$. The physical meaning of the parameter Z_m is discussed in the appendix.

We define here the exact value of $\widetilde{\lambda}_{\mathrm{d}}$ for $a_{\mathrm{c}} \neq 0$ by considering an interesting property of the twist defects first found numerically by Kopp and Genack [3], namely the fact that for $\lambda = \widetilde{\lambda}_{\mathrm{d}}$ the defect plane totally reflects the eigenwaves $2^{\pm}$. For this purpose it is enough to consider the solution defined at point (i) of 3.1, corresponding to a field in which the eigenwave 1^- is absent in b, and search for the value $\widetilde{\lambda}_{\mathrm{d}}$ of $\widetilde{\lambda}$ which makes equal to zero the amplitude of the eigenwave 1^+ in b. Straightforward calculations give the following relation between θ and $\widetilde{\lambda}_{\mathrm{d}}$,

$$\theta = \cot^{-1}\left[\frac{\mathrm{i}}{2}\left(\frac{u_2\left(u_1\varepsilon_1 + 2\varepsilon_m\widetilde{\lambda}_{\mathrm{d}}^2\right)}{4n_1u\varepsilon_m\widetilde{\lambda}_{\mathrm{d}}} - \frac{2n_1u_1\varepsilon_m\widetilde{\lambda}_{\mathrm{d}}}{u\left(u_1\varepsilon_1 + 2\varepsilon_m\widetilde{\lambda}_{\mathrm{d}}^2\right)}\right)\right] + m\pi, \tag{23}$$

where m is any integer, since θ is defined modulus π. We have found numerically that this equation is completely equivalent to the equation given in [2][5] for $\widetilde{\lambda}_{\mathrm{d}}$ and that the approximation given by equation (22) is in any case quite good, as shown in figure 2.

3.3. Thin samples

When the thickness $2l$ of the sample is comparable with the attenuation length l_{d} of the modes $1^{\pm}$, all the eigenwaves can reach the defect plane. Thus, it is impossible to define all the elements of the scattering matrix using the solutions given by equations (19) and (20) where only three of the four eigenwaves are considered. According to the standard procedure [18], we consider first the *transfer matrix* (or *propagator*) U, which is, implicitly defined by the

[5] But in [2], the twist angle is defined by considering the opposite rotation, so that it has the opposite value.

equation $\alpha_b(0^+) = U\alpha_a(0^-)$. Taking into account equation (18), the relation $\beta = T\alpha$, and the continuity of $\beta(z)$ at the defect site $z = 0$, one obtains

$$U = U(0^+, 0^-) = T^{-1}\exp(-R\theta)T \equiv \cos\theta\,\mathbf{I} - \sin\theta\,R_S, \tag{24}$$

where

$$R_S = T^{-1}RT.$$

The matrix R_S is similar to the matrix R defined in equation (4). Therefore: $R_S^{-1} = -R_S$ and their determinant is equal to 1. To find the elements of R_S we express T^{-1} as a function of T using the relation $G_\alpha = T^\dagger G_\beta T$ of section 2.2 and the equations defining the elements of T, G_α and G_β. Straightforward calculations give

$$R_S = \begin{pmatrix} -r_1 & -r_5^* & -r_3 & -r_5 \\ \mathrm{i}r_5^* & \mathrm{i}r_2 & \mathrm{i}r_5 & \mathrm{i}r_4 \\ r_3 & r_5 & r_1 & r_5^* \\ -\mathrm{i}r_5 & -\mathrm{i}r_4 & -\mathrm{i}r_5^* & -\mathrm{i}r_2 \end{pmatrix} \tag{25}$$

where the quantities r_j $(j = 1, \ldots, 5)$ are

$$\begin{aligned} r_{1,3} &= 2\widetilde{\lambda}c_1^2\big[(2\widetilde{\lambda}^2\varepsilon_m + u_1\varepsilon_1)(u_2 - 2\varepsilon_1\mu_m) \mp 2n_1^2u_1\varepsilon_m\big], \\ r_{2,4} &= 2\widetilde{\lambda}c_2^2\big[(2\widetilde{\lambda}^2\varepsilon_m + u_2\varepsilon_1)(u_1 - 2\varepsilon_1\mu_m) \mp 2n_2^2u_2\varepsilon_m\big], \\ r_5 &= 4\widetilde{\lambda}c_1c_2a_c(\varepsilon_1(a_c - \varepsilon_1\mu_m) + \varepsilon_m(\widetilde{\lambda}^2 + n_1n_2)), \end{aligned} \tag{26}$$

and satisfy the relation $r_3^2 + r_4^2 = r_1^2 + r_2^2$.

The derivation of the scattering matrix from U is standard [18]. It is convenient to write the 4×4 matrix U as

$$U = \begin{pmatrix} U_{\mathrm{ff}} & U_{\mathrm{fb}} \\ U_{\mathrm{bf}} & U_{\mathrm{bb}} \end{pmatrix}, \tag{27}$$

where f and b stand for forward and backward, respectively, and to consider also the matrix $U^{-1} \equiv \cos\theta\,\mathbf{I} + \sin\theta\,R_S$. The 2×2 matrix S_{ff} is the inverse of $(U^{-1})_{\mathrm{ff}}$, that is given by

$$(U^{-1})_{\mathrm{ff}} = \begin{pmatrix} \cos\theta - r_1\sin\theta & -r_5^* \\ \mathrm{i}r_5^* & \cos\theta + \mathrm{i}r_2\sin\theta \end{pmatrix}. \tag{28}$$

As already stated, for $\widetilde{\lambda} = \widetilde{\lambda}_d$ the eigenwave 2^+ is totally reflected at the defect plane. This means that the element $(2, 2)$ of S, which coincides with the element $(2, 2)$ of S_{ff}, is equal to zero. It is easy to show that this element is zero when the element $(1, 1)$ of its inverse matrix $(U^{-1})_{\mathrm{ff}}$, given by equation (28), is zero (see section 6.2). Therefore, the quantity $\widetilde{\lambda}_d$ is implicitly defined by the equation

$$\theta = \cot^{-1}[r_1(\widetilde{\lambda}_d)] + m\pi, \tag{29}$$

which is fully equivalent to equation (23).

The reflectance and transmittance of the sample are defined by the scattering matrix of the whole sample. Its computation is again standard [18]. The curves giving the dependence on λ of these quantities for different values of l, θ, a_c and for the different polarization states have already been found numerically in [2, 3, 6] and will not be reported here. We remark only that such curves display enhanced maxima or minima for $\widetilde{\lambda} \approx \widetilde{\lambda}_d$, whose spectral width $\Delta\omega$ is equal to τ^{-1}, where τ is the decay time of defect mode. When $l \gg l_d$, where l_d is the attenuation length of the eigenwaves $1^\pm$, τ is practically independent of l but depends drastically on a_c, since the energy stored by the defect mode can only escape because of the presence of the nonlocalized component. For $a_c = 0$ such component disappears, τ goes to infinite and $\Delta\omega$ goes to zero. We finally mention that dissipation in lossy media has dramatic effects on $\Delta\omega$ and gives rise to paradoxical effects [2, 10].

4. Doublets

We consider now an unbounded helical medium with two identical twist defects at $z = 0$ and $z = z_1$. The transfer matrix relating the α-vectors at $z = 0^-$ and $z = z_1^+$ is given by

$$U = U\left(z_1^+, 0^-\right) = U_1 \exp(\mathrm{i}Nz_1)\, U_1 \tag{30}$$

where U_1 is the transfer matrix for each one of the defect planes, given by equation (24), and N is the diagonal matrix with diagonal elements equal to n_j. The matrix $\exp(\mathrm{i}Nz_1)$ is the transfer matrix $U(z_1^-, 0^+)$ of the layer between the two twist defects.

4.1. Scattering properties of the layer with two twist defects

The scattering matrix $S = S\left(z_1^+, 0^-\right)$ can be written as

$$S = (P_1 - U\,P_2)^{-1}(U\,P_1 - P_2). \tag{31}$$

where P_1 and P_2 are the diagonal matrices defined as

$$\begin{pmatrix} 1 & 0 & 0 & 0 \\ 0 & 1 & 0 & 0 \\ 0 & 0 & 0 & 0 \\ 0 & 0 & 0 & 0 \end{pmatrix} \qquad \text{and} \qquad \begin{pmatrix} 0 & 0 & 0 & 0 \\ 0 & 0 & 0 & 0 \\ 0 & 0 & 1 & 0 \\ 0 & 0 & 0 & 1 \end{pmatrix},$$

respectively ($P_1\alpha$ and $P_2\alpha$ represent therefore the forward and backward components of α, respectively). The element (i, j) of S correspond to waves incident from the left when $j = (1, 2)$ and give the transmission and reflection properties of the layer when $i = (1, 2)$ and $i = (3, 4)$, respectively (we recall that the vector α defines the amplitude of the four eigenwaves in the order $1^+, 2^+, 1^-, 2^-$). The square amplitudes of such elements give the transmittance and reflectance of the layer for waves incident from the left. The curves giving such quantities versus $\widetilde{\lambda}$ are quite similar to the corresponding curves found in [2, 3, 6] for a single twist defect, except for the fact that they have the structure of a doublet with two defect frequencies $\widetilde{\lambda}_{\mathrm{d}1}, \widetilde{\lambda}_{\mathrm{d}2}$. The curves $(1, 1)$ and $(2, 2)$ giving the transmittance for the eigenmodes 1 and 2, respectively, are plotted in figure 3. For $\widetilde{\lambda} = \widetilde{\lambda}_{\mathrm{d}1}$ and $\widetilde{\lambda} = \widetilde{\lambda}_{\mathrm{d}2}$ the eigenwave 1 generates at the other side of the layer an eigenwave 1 with a huge amplitude, whereas the eigenwave 2 is totally reflected since the transmitted curve is completely absent. We recall that a single twist defect reflects totally the eigenwave 2 only for $\widetilde{\lambda} = \widetilde{\lambda}_{\mathrm{d}}$, where $\widetilde{\lambda}_{\mathrm{d}}$ is between $\widetilde{\lambda}_{\mathrm{d}1}$ and $\widetilde{\lambda}_{\mathrm{d}2}$. The presence of the other defect drastically changes this reflection property.

The behaviours of the other curves, not plotted here, can be summarized as follows. They display enhanced peaks with the same spectral width as the curves plotted in figure 3. The peak value of the curve $(3, 1)$ is nearly equal to the peak value of the curve $(1, 1)$. This mean that the eigenmode 1 generates huge eigenmodes 1 also in reflection. The mixed curves, giving the square amplitudes of the eigenwaves 1 generated by the eigenwave 2 and vice versa, show peaks whose peak values are smaller (they are roughly equal to the square root of the $(1, 1)$ peak). The fact that a single wave with unit amplitude incident on the layer can generate reflected and transmitted waves with huge amplitude could be surprising, but the energy is in any case conserved.

4.2. Defect frequencies

The defect frequencies $\widetilde{\lambda}_{\mathrm{d}1}, \widetilde{\lambda}_{\mathrm{d}2}$ can be found using the same procedure of section 3.3. Figure 3 shows that at the defect frequencies the element $(2, 2)$ of the matrix S is equal to zero, a fact

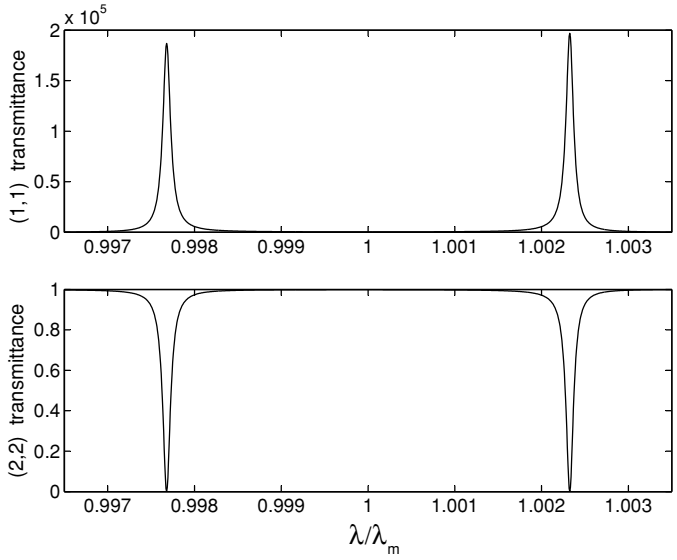

Figure 3. Transmittance of the layer including two identical twist defects versus the reduced wavelength $\widetilde{\lambda}/\widetilde{\lambda}_m$ for the eigenwaves 1 (upper curve) and 2 (lower curve) for $\varepsilon_1 = 3, \varepsilon_2 = 3.6$, $\mu_1 = \mu_2 = 1, \theta = \pi/2, z_1 = 3l_\mathrm{d}$. At the defect frequencies the eigenwave 1^+ generates an eigenwave 1^+ with a huge amplitude at the other side of the layer, whereas the eigenwave 2^+ is totally reflected, since the transmittance is zero.

which implies that the element (1, 1) of the matrix U^{-1} is zero. Setting to zero, one obtains this element easily,

$$\cot\theta = r_1 \pm \exp(-z_1/(2l_\mathrm{d}))\left(r_3^2\exp(-z_1/l_\mathrm{d}) + 2\,\mathrm{Im}\left(r_5^2\exp(\mathrm{i}n_2z_1)\right)\right)^{1/2}, \tag{32}$$

which is satisfied by two different values $\widetilde{\lambda}_{\mathrm{d}1}, \widetilde{\lambda}_{\mathrm{d}2}$ of $\widetilde{\lambda}$ for any value of θ (note that the quantities $l_\mathrm{d} \equiv 1/|n_1|$, r_3, r_5 and n_2 are the functions of $\widetilde{\lambda}$). The terms containing the common factor $\exp(-z_1/(2l_\mathrm{d}))$ act here as perturbing terms. For $z_1 \gg l_\mathrm{d}$ such terms vanish and equation (32) becomes identical to equation (29), which gives the frequency $\widetilde{\lambda}_\mathrm{d}$ of the singlet. In other words, when the two twist defects are very much separated, they act independently with each other and the two defect modes becomes degenerated, since $\widetilde{\lambda}_{\mathrm{d}1} = \widetilde{\lambda}_{\mathrm{d}2} = \widetilde{\lambda}_\mathrm{d}$. We recall that l_d is the attenuation length of the eigenwaves $1^\pm$, which constitute the dominant components of the defect modes and are localized near the defect planes. When $z_1 \gg l_\mathrm{d}$, the component peaked at $z = 0$ does not reach the defect plane $z = z_1$, and vice versa. This fact suggests that the 'interaction' between the two defects is mainly due to the localized components of the defect modes, which in equation (32) is represented by the first one of the two perturbing terms. Neglecting the other term, equation (32) assumes the simple form,

$$\cot\theta = r_1 \pm r_3\exp(-z_1/l_\mathrm{d}), \tag{33}$$

which gives the defect frequencies with a good approximation (within 0.1% for reasonable values of the material parameters).

For $a_\mathrm{c} = 0$ the continuity conditions of the vectors **e** and **h** at the two defect planes can be satisfied by considering only the eigenmodes $1^\pm$, for the same reasons discussed in section 3.2 (see figure 4). The defect modes contain only the eigenwave 1^- for $z < 0$ (region a), both eigenwaves 1^+ and 1^- in region b ($0 < 0 < z_1$), and the eigenwave 1^+ in region c ($z > z_1$). Only the vectors **e** are considered in figure 4 because for $a_\mathrm{c} = 0$ the continuity of **e** implies the

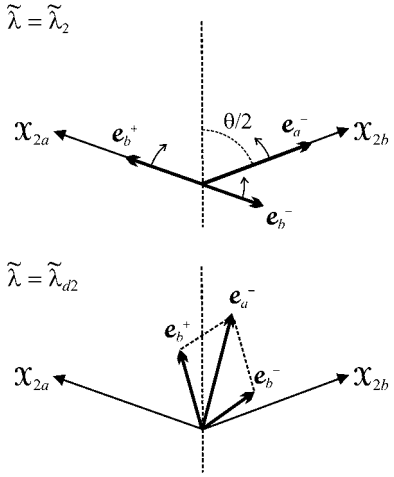

Figure 4. Rotation of the vectors **e** at the two sides a, b of the twist plane $z = 0$. For $a_c = 0$ the continuity conditions for the vectors **e**, **h** can be satisfied by considering only the modes $1^{\pm}$. For $\widetilde{\lambda} = \widetilde{\lambda}_2$ (upper figure), the vectors $\mathbf{e}_a^-$ and $\mathbf{e}_b^+$ are parallel to x_{2a} and x_{2b}, but in the region b we have also a vector $\mathbf{e}_b^-$, due to the presence of the other twist defect. The defect wavelengths $\widetilde{\lambda}_{d1}, \widetilde{\lambda}_{d2}$ of the two twist modes correspond to $\mathbf{e}_b^-$ parallel and antiparallel, respectively, to $\mathbf{e}_b^+$. We consider here the second case. The lower figure shows how the boundary condition $\mathbf{e}_b^+ + \mathbf{e}_b^- = \mathbf{e}_a^-$ can be satisfied and suggest that this occurs after a rotation $\phi < \theta/2$. This implies that $\widetilde{\lambda}_{d2}$ is intermediate between $\widetilde{\lambda}_2$ and de defect frequency $\widetilde{\lambda}_d$ of samples with only one twist defect, since $\widetilde{\lambda} = \widetilde{\lambda}_d$ when $\phi = \theta/2$.

continuity of **h**, which is parallel to **e**. The figure clearly explains the presence of two different defect modes and suggests that the quantities $\widetilde{\lambda}_2, \widetilde{\lambda}_{d2}, \widetilde{\lambda}_d, \widetilde{\lambda}_{d1}$, and $\widetilde{\lambda}_1$ are in decreasing order (thus, the corresponding frequencies are in increasing order).

The curves giving the square amplitudes of the elements of the scattering matrix $S\left(z_1^+, 0^-\right)$ versus $\widetilde{\lambda}$ are strongly asymmetric. They could be quite symmetric only in the particularly interesting case $\theta = \pi/2$. This is shown in figure 5, which gives the $(1, 1)$ transmittance for different values of the distance z_1 between the defect planes. The separation $\widetilde{\lambda}_{d2} - \widetilde{\lambda}_{d1}$ between the peaks decreases by increasing z_1. We have found that for $\theta = \pi/2$ and $a_c = 0$, this separation is approximately given by the simple equation

$$\widetilde{\lambda}_{d2} - \widetilde{\lambda}_{d1} = (\widetilde{\lambda}_2 - \widetilde{\lambda}_1) \exp(-z_1/l_d) \tag{34}$$

where $l_d = 1/|n_1|$ and $n_1 = n_1(\widetilde{\lambda}_{d1}) = n_1(\widetilde{\lambda}_{d2})$. The degree of validity of equation (34), shown in figure 6 does not depend greatly on the material parameters $\varepsilon_1, \varepsilon_2, \mu_1, \mu_2$.

Finally, we observe that the equation giving the defect frequency for two twist defects with opposite rotations is

$$\cot^2\theta = r_1^2 - \exp(-z_1/(l_d))\left(r_3^2 \exp(-z_1/l_d) - 2\,\mathrm{Im}\left(r_5^2 \exp(\mathrm{i}n_2 z_1)\right)\right). \tag{35}$$

4.3. Finite samples

We discuss here the scattering properties and the polarization of the internal field in finite samples with two twist defects which divide the whole sample in the regions, a for $(-z_a < z < 0), b$ for $(0 < z < z_1)$, and c for $(z_1 < z < z_c)$, where z_a and z_c define the sample boundaries. In order to explain the behaviours of the scattering curves is worthwhile

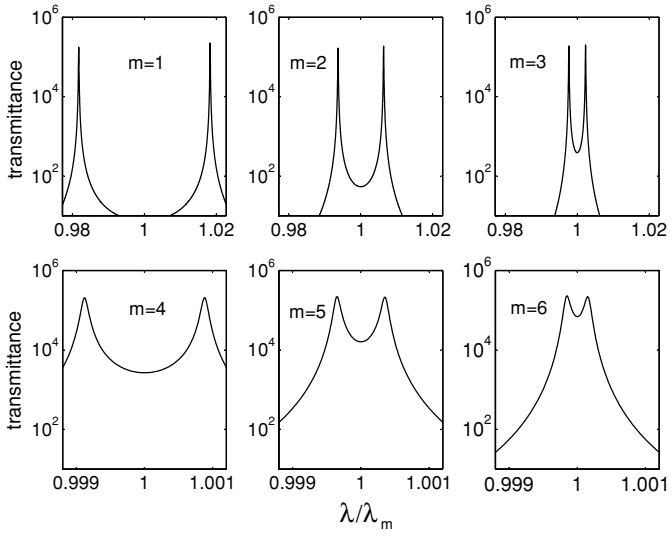

Figure 5. (1, 1) Transmittance curves versus the reduced wavelength $\widetilde{\lambda}/\widetilde{\lambda}_m$ for $z_1 = ml_d$ where l_d is the attenuation length of the eigenwaves $1^{\pm}$ and $m = 1, 2, 3, 4, 5, 6$. The other parameters are the same as in figure 3. Notice the scale change for the x-axis in the lower curves.

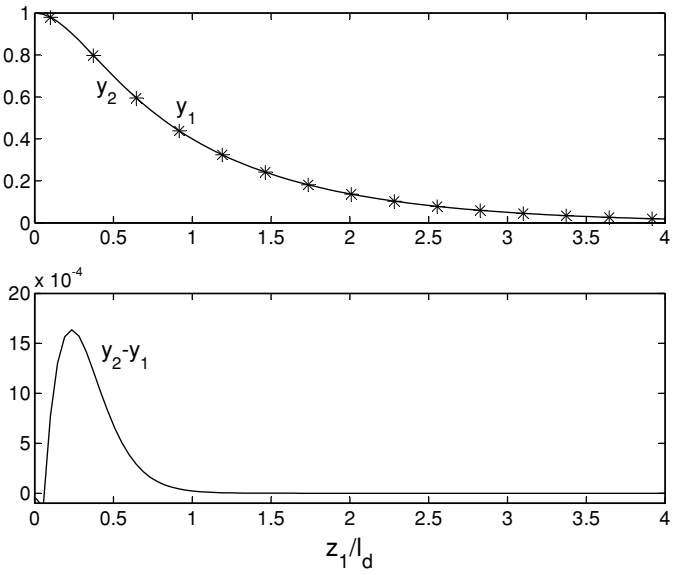

Figure 6. A comparison between the exact (y_1) and approximate (y_2) values of the peak separation versus the normalized distance $z_1/l_d : y_1 = (\widetilde{\lambda}_{d2} - \widetilde{\lambda}_{d1})/(\widetilde{\lambda}_2 - \widetilde{\lambda}_1)$ (stars); $y_2 = \exp(-z_1/l_d)$ (full line). The parameters are the same as in figure 3. In the limit $z_1 = 0$ the peaks are shifted at the band edges, that is $\widetilde{\lambda}_{d1} = \widetilde{\lambda}_1$ and $\widetilde{\lambda}_{d2} = \widetilde{\lambda}_2$, since $y_1 = 1$.

to remark that an external wave incident from the left generates the internal eigenwaves 1^+, 2^+ at the first boundary plane ($z = -z_a$). When the impedance mismatch between the external medium and the helical structure is small, circularly polarized waves generate practically only one of such eigenwaves. In the right-handed helices considered here, right (rcp) and left (lcp)

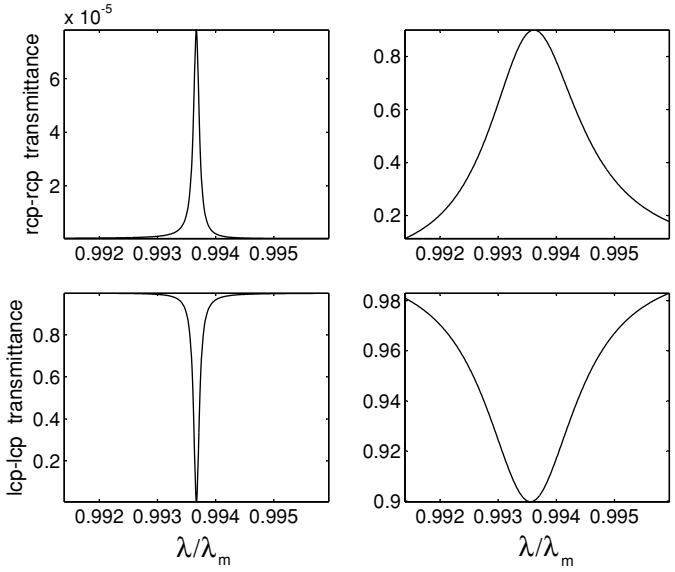

Figure 7. Transmittance curves near the first defect frequency for right circularly polarized waves (rcp, upper curves) and left circularly polarized waves (lcp, lower curves) in a thick sample (left side curves) and a thin one (right side curves). The material parameters and the twist angle are the same as in figure 3. The sample boundaries are at $z = -z_a$ and $z = z_1 + z_a$, the twist defects at $z = 0$ and $z = z_1$, where $z_1 = 2l_d$ in both samples, z_a is $6l_d$ and $2l_d$ in the thick and the thin samples, respectively. The properties of the curves (thickness and height of peaks and holes) is discussed in the text.

polarizations generate the eigenwaves 1^+ and 2^+, respectively. In contrast, a wave incident on a defect plane generates all the eigenwaves, two reflected and two transmitted, because the mismatch is very large.

In figure 7, we have plotted the transmittance curves of two samples with the same material parameters and the same defect frequencies but with a different thickness, in order to exhibit the main role of sample size. The most evident difference concerns the width of peaks and holes. In the thick sample (left curves, $z_a = z_c = 6l_d$, $z_1 = 2l_d$ where l_d is the attenuation length of the eigenwaves $1^\pm$) the width is practically the same as for the curves giving the square amplitudes of the element of the scattering matrix $S\left(z_1^+, 0^-\right)$. In fact when both z_a and z_c are much larger than l_d only the nonlocalized component reaches the sample boundary. Since in lossless media the amplitude of such component is independent of z, the energy loss, the decay time, and the line widths remain unchanged. The decay time begins to decrease (and the line width to increase) when at least one of the parameters z_a, z_c is such that the amplitude of the localized components at the sample boundary is no more negligibly small. The upper curves show that a right circularly polarized wave, which generates the eigenwave 1^+, is transmitted only near its defect frequency. In fact within any one of the three regions, the eigenwave 1^+ drastically reduces its intensity, but at the defect frequency it is greatly enhanced when it reaches a defect plane. This mechanism implies that a sample with any thickness can transmit the attenuated eigenwave 1^+ if we insert many twist defects in the sample at a distance comparable with l_d. The lower curves show that the twist defects no longer reflect totally the eigenwaves 2^+ for thin samples.

The main properties of the internal electromagnetic field generated by an lcp wave with unit power flux in the same thick sample as in figure 7 are shown in figure 8. The polarization

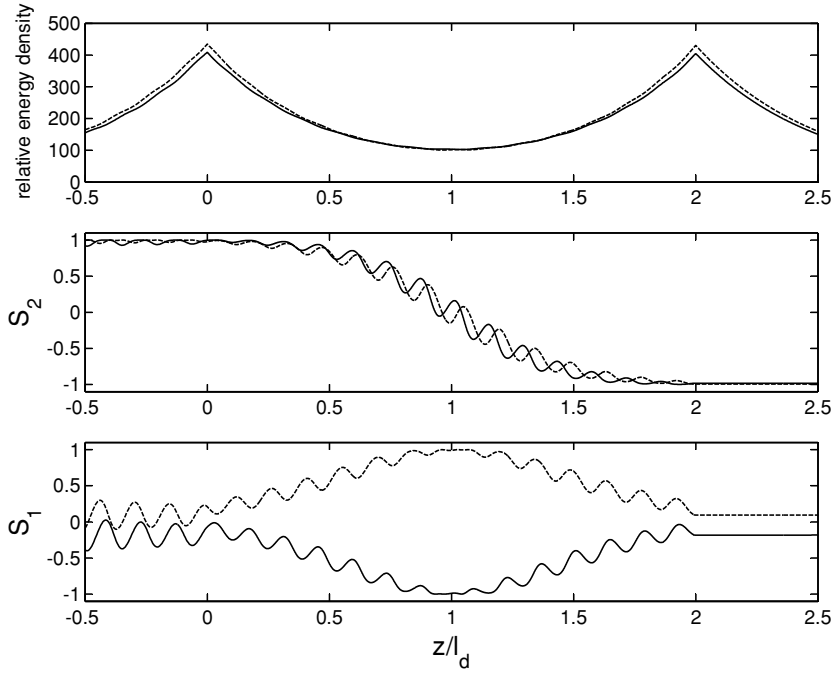

Figure 8. Properties of the internal field generated by a left circularly polarized wave with unit energy density incident from the left and the thick sample considered in figure 7. The curves refer to the central part of the sample, which includes the twist defects (at $z = 0$ and $z = z_1 = 2l_d$). The upper curves show that the relative energy density is maximum at the defect planes, as expected. The lower curves define the polarization properties of the two defect modes, whose reduced wavelengths $\widetilde{\lambda}$ are $\widetilde{\lambda}_{d1} = 0.9937\widetilde{\lambda}_m$ (full lines) and $\widetilde{\lambda}_{d2} = 1.0066\widetilde{\lambda}_m$ (dotted lines). The meaning of the Stokes parameters s_1 and s_2 is defined in the text.

properties of the field are defined by the Stokes parameters s_1, s_2, s_3, that is, by a point on the Poincaré sphere. The curves giving s_3 are omitted since this parameter is very small in the whole z-interval. This means that the polarization of the internal field is nearly linear everywhere. The angle between the electric field **e** and the axis x_1 is nearly equal to 45° around the first twist defect (where s_2 is nearly equal to +1 and s_2 is small), and nearly equal to −45° around the other twist defect ($s_2 \approx -1$, $s_1 \approx 0$). The vectors **e** rotate by almost ±90° in the region between the defect planes. At the midpoint of this region they are nearly parallel to x_1 ($s_1 \approx 1$) or to x_2 ($s_1 \approx -1$). The undulation is due to the presence of the small components $2^{\pm}$, which interfere with the dominant components $1^{\pm}$. The absence of this undulation in the region c ($z > z_1 = 2l_d$) means that the eigenwaves $2^{\pm}$ are practically absent in this region, confirming the fact that the thick sample reflects totally the incident *lcd* wave (the relative energy density at the second sample boundary is nearly equal to 0.005).

5. Multiplets

The equation giving the transfer matrix for n_0 identical and equidistant twist defects at $z = nz_1$, where $n = 0, 1, 2, \ldots, n_0 - 1$, can be written as

$$U = U\left((n_0 - 1)z_1^+, 0^-\right) = U_1[(\exp(\mathrm{i}Nz_1))U_1]^{n_0-1}. \tag{36}$$

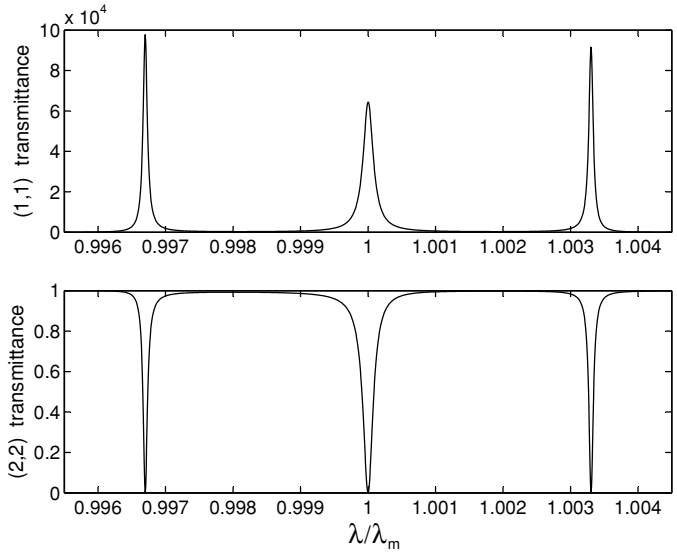

Figure 9. Transmittance of the layer including $n_0 = 3$ identical twist defects versus the reduced wavelength $\widetilde{\lambda}/\widetilde{\lambda}_m$ for the eigenwave 1 (upper curve) and 2 (lower curve) $\theta = \pi/2$, $z_1 = 3l_d$, and the values of the other parameters are the same as figure 3. Here transmittance does not refer to the ratio between the energy flux of the transmitted and incident waves, which for the standing eigenwaves 1 is zero, but to their energy densities.

For $n_0 = 2$, equation (36) becomes identical to equation (30). The square amplitudes of the elements (1, 1) and (2, 2) of the scattering matrix are plotted in figure 9 for $N = 3$, $\theta = \pi/2$ and $z_1 = 3l_d$. The figure shows three different twist defects at the wavelengths $\widetilde{\lambda}_{d1}$, $\widetilde{\lambda}_{d2}$, $\widetilde{\lambda}_{d3}$, where $\widetilde{\lambda}_{d2}$ is nearly equal to the average value of $\widetilde{\lambda}_{d1}$, $\widetilde{\lambda}_{d3}$. At the defect frequencies, the structure totally reflects the eigenwave 2. This allows us to define the defect frequencies by setting to zero the element (1, 1) of the matrix U^{-1}. In the particular case $a_c = 0$ the twist defects contain only the localized eigenwaves $1^{\pm}$ for any value of n_0 and the defect frequencies can be found using 2×2 matrices (see the appendix). For three identical and equidistant defects, this gives

$$\frac{(\cot\theta - r_1)^3}{r_3^2} = (\cot\theta - r_1)(\exp(-2z_1/l_d) + \exp(-4z_1/l_d) + \exp(-6z_1/l_d)) + 2r_1\exp(-6z_1/l_d). \tag{37}$$

For any value of $\widetilde{\lambda}$ within the band gap, equation (37) gives three different values for the twist angle θ in the interval $[0, \pi]$. This fact justifies that for any given θ it admits three different values for $\widetilde{\lambda}$ within the band gap.

Transmittance curves for $n_0 = 5$ are depicted in figure 10. They have shown that the different twist defects have different heights and widths even for the particularly symmetric case $\theta = \pi/2$.

6. Comments and concluding remarks

In section 2 we have defined (1) the Hilbert space of the state vectors for the electromagnetic field generated within the sample by the incident waves, (2) the four eigenwaves of the periodic structure without defects and (3) a scalar product having a simple physical meaning. With

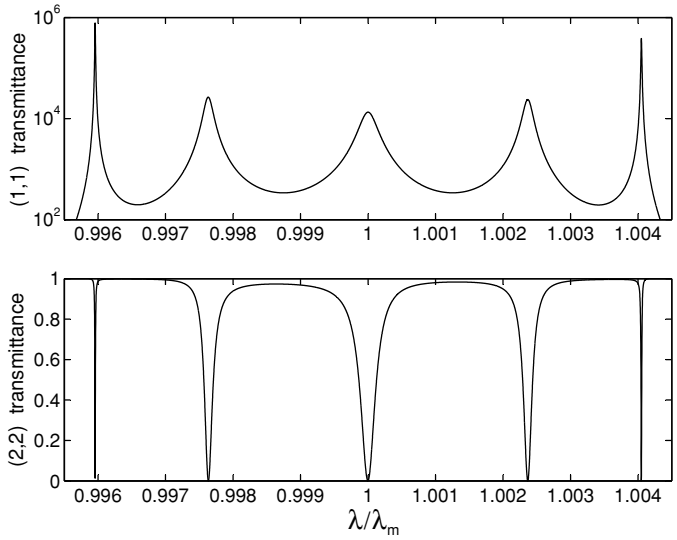

Figure 10. The same as figure 9 but for $n_0 = 5$ identical twist defects. For the sake of clarity, we used a semi-logarithmic scale on the top panel.

these definitions, it becomes quite easy to compute the scattering properties of samples with any number of twist defects. Many interesting properties have been found numerically, but a purely numerical approach is of little help for their understanding. Hence our effort to find analytic expressions and equations, and more generally to get a deeper insight into the physics of the problem. We add here some comments about further developments and applications and to provide a better explanation of some particularly interesting properties.

6.1. Periodic helical structures and homogeneous chiral media

In the frame x_1, x_2, x_3 rotating solidly with the tensors ε and μ, the propagation equation of the electromagnetic field within the helical structure becomes the same as in an *homogeneous* medium. Since the considered defects are spaceless, reducing to discontinuity planes within the medium, our problem becomes identical to the well-known problem of the wave propagation in a set of homogeneous layers separated by discontinuity planes. The 'equivalent' homogeneous medium is anisotropic and chiral. The chiral parameter here is the helix pitch p, which is related to the quantity $\widetilde{\lambda} = \lambda/p$ and plays exactly the same role as the chiral parameter k in an isotropic medium [19].

Therefore, the equations which define the eigenvalues and eigenvectors of **H** are valid also for the equivalent homogeneous medium by simply substituting p with k. The most surprising consequence of this analogy is due to the fact that a band gap may appear also in homogeneous media. Such important point deserves some comments. The equivalent homogeneous medium is isotropic for its chiral properties, since only one chiral parameter appears, and anisotropic for the other properties. This is quite unusual. If we consider a medium which is isotropic for all its properties the band gap disappears since its edges $\lambda_1 = k\sqrt{\varepsilon_1\mu_1}$ and $\lambda_2 = k\sqrt{\varepsilon_2\mu_2}$ coincide. However, the most important point is the following one. In helical media p can have any value, whereas in most chiral media the actual value of k is such that λ_1 and λ_2 are very small (of the order of the molecular size). For such λ-values the analogy could fail. In fact the continuum models used in the macroscopic approaches, which neglect the molecular

structure of matter, are valid only for λ-values greater the molecular size. In conclusion, the possibility that the theory developed here could be useful also for homogeneous media is not excluded but it deserves further research.

Owing to the analogy between homogeneous media and the periodic structures considered here, it is not surprising that it has been possible to find exact analytic expressions for such structures, which play therefore an unique role among periodic media (nothing similar is possible for any other periodic structure with defects). This is a good reason for their study, in our opinion. The main difference between the equations given here and the equations found in the literature for homogeneous media is due to the fact that we are interested to solutions within the frequency gap, which to our knowledge are not yet been considered in the optics of homogeneous media. From the point of view of applications, the main difference between the helical structures and the other 1D crystals concerns their polarization properties. In fact the presence of a chirality parameter makes the polarization of the eigenwaves nearly circular, whereas in most anisotropic media it is linear or nearly linear.

We finally recall that the helical medium appears homogeneous and admits plane-wave solutions only in the rotating frame. In the laboratory frame, the solutions are obviously Bloch waves.

6.2. Scattering properties and defect frequency

In section 3.3, we have defined the defect wavelength $\widetilde{\lambda}_{\mathrm{d}}$ of a sample with only one twist defect by setting to zero the element (2, 2) of the scattering matrix. Such definition deserves some comments.

For the definition of $\widetilde{\lambda}_{\mathrm{d}}$ it is reasonable to consider the scattering properties of the sample, because the curves $f_{ij}(\widetilde{\lambda}) = |S_{ij}(\widetilde{\lambda})|^2$, where S_{ij} are the elements of the scattering matrix, display enhanced maxima or minima only in the presence of defects. The definition of $\widetilde{\lambda}_{\mathrm{d}}$ becomes obvious if and only if all the maxima and minima occur at the same $\widetilde{\lambda}$-value. A numerical analysis shows that this not the case in general, but it is not easy to have an intuitive feeling of the origin of the difference between the position of two different peaks. In fact, to define the matrix S we must first compute the transfer matrix U, whose elements depend very smoothly on $\widetilde{\lambda}$ even in the presence of defects. In section 3.3, we have set to zero the element (1, 1) of the inverse transfer matrix, which is given by expression (28). In this case, the quantities f_{ij} giving the transmittances of the defect plane are

$$f_{11} = \left(\cos^2\theta + r_2^2 \sin^2\theta\right)\big/|r_5|^4, \qquad f_{12} = f_{21} = 1/|r_5|^2, \qquad f_{22} = 0. \tag{38}$$

The quantity r_5 defined by equation (26), contains the factor a_{c}. Thus, the quantities f_{11}, f_{12}, f_{21} diverge when a_{c} goes to zero. In this case the defect frequency is defined without any ambiguity because the functions $f_{ij}(\widetilde{\lambda})$ become proportional to the Dirac function $\delta(\widetilde{\lambda}-\widetilde{\lambda}_{\mathrm{d}})$. In the general case $a_{\mathrm{c}} \neq 0$ the peaks and holes of the functions $f_{ij}(\widetilde{\lambda})$ have a finite thickness and their maxima and minima occur at different $\widetilde{\lambda}$-values, but the differences between such values is small when the modulus of a_{c} is small. For typical values of the anisotropy parameters the differences are so small that we can choose any one of these values as a possible definition of $\widetilde{\lambda}_{\mathrm{d}}$. We have chosen the minimum of f_{22} because it is defined by a simpler equation. In conclusion, the defect frequency can be defined exactly, without any ambiguity, only when $a_{\mathrm{c}} = 0$ and in actual samples it is quite well defined because a_{c} is a small parameter.

Here, we have considered the scattering matrix of the defect plane for the *internal* eigenwaves. The interest of our analysis may appear purely academic, because in experiments only finite samples and *external* waves are considered. Obviously the maxima or minima of such curves occurs again at a well-defined frequency only when $a_{\mathrm{c}} = 0$. This fact confirms

the main role of the parameter a_c for the optical properties of samples with twist defects. We recall that in nonmagnetic media the width of the frequency gap is zero when $a_c = 0$. Thus, it has been possible to use a_c as a free parameter, in order to better understand its role, because the considered medium is both dielectric and magnetic.

Acknowledgment

We acknowledge support from CONACYT México, Grant No. 41035 and DGAPA IN112503.

Appendix. Material parameters and scaling laws

The parameters defining the helical structure without defects are $\varepsilon_1, \varepsilon_2, \mu_1, \mu_2$, and the helix pitch p. The last quantity does not appear in our equations because we have used the reduced wavelength $\widetilde{\lambda} = \lambda/p$. This fact implies that the properties discussed in the paper do not depend separately on λ and p but only on the ratio λ/p: a change of p simply *rescales* the wavelengths defining the width of the band gap and the defect frequencies. It seems interesting to search for other possible *scaling* laws. To this aim we have rewritten all the found equations using the new sets of parameters:

$$\widetilde{\lambda}_1 = \sqrt{\varepsilon_1\mu_1}, \qquad \widetilde{\lambda}_2 = \sqrt{\varepsilon_2\mu_2}, \qquad Z_1 = \sqrt{\mu_1/\varepsilon_1}, \qquad Z_2 = \sqrt{\mu_2/\varepsilon_2}, \tag{A.1}$$

and

$$\begin{aligned} &\widetilde{\lambda}_m = (\widetilde{\lambda}_1 + \widetilde{\lambda}_2)/2, \qquad \widetilde{\lambda}_a = (\widetilde{\lambda}_2 - \widetilde{\lambda}_1)/2, \\ &Z_m = (Z_1 + Z_2)/2, \qquad Z_a = (Z_2 - Z_1)/2; \end{aligned} \tag{A.2}$$

instead of the material parameters $\varepsilon_1, \varepsilon_2, \mu_1, \mu_2$. The found results can be summarized as follows.

(i) By setting $x = \widetilde{\lambda}/\widetilde{\lambda}_m$, the equation defining the defect modes and their properties depend only on the ratios

$$x_a = \widetilde{\lambda}_a/\widetilde{\lambda}_m, \qquad z_a = Z_a/Z_m. \tag{A.3}$$

Only two of the four material parameters are independent, a fact that gives other two scaling laws.

The parameter x_a defines the relative width of the band gap, the parameter z_a defines the width of the defects lines and plays therefore the same role as the anisotropy parameter a_c, which can be written as

$$a_c = 2\frac{1 - x_a^2}{1 - z_a^2}\widetilde{\lambda}_m^2 z_a. \tag{A.4}$$

(ii) The parameters Z_1 and Z_2 play the role of impedances for the eigenwaves $1^{\pm}$. In fact at the band edge $\widetilde{\lambda} = \widetilde{\lambda}_1$, the ratio $|\mathbf{e}_1|/|\mathbf{h}_1|$ is equal to $Z_1 = \sqrt{\mu_1/\varepsilon_1}$ since both vectors $\mathbf{e}_1$ and $\mathbf{h}_1$ are parallel to x_1. The same occurs at the other band edge, with the suffix 2 instead of 1. When $a_c = z_a = 0$, $Z_1 = Z_2$ and $|\mathbf{e}_1|/|\mathbf{h}_1| = |\mathbf{e}_2|/|\mathbf{h}_2|$, a fact which helps us to understand why for $a_c = 0$, the vectors $\mathbf{e}$ and $\mathbf{h}$ rotate rigidly within the band gap, by keeping parallel to each other.

(iii) When $a_c = z_a = 0$, the quantity r_5 appearing in the matrices R_S and U, equations (24) and (25), respectively, is identically zero. If we write the eigenwaves $1^{\pm}, 2^{\pm}$ in the order $1^+, 1^-, 2^+, 2^-$ the transfer matrix U of the defect plane becomes

$$U = \begin{pmatrix} U_{11} & 0 \\ 0 & U_{22} \end{pmatrix}, \tag{A.5}$$

where

$$U_{11} = \begin{pmatrix} 1 & 0 \\ 0 & 1 \end{pmatrix} \cos\theta - \begin{pmatrix} -r_1 & -r_3 \\ r_3 & r_1 \end{pmatrix} \sin\theta,$$
$$U_{22} = \begin{pmatrix} 1 & 0 \\ 0 & 1 \end{pmatrix} \cos\theta - \mathrm{i} \begin{pmatrix} r_2 & r_4 \\ -r_4 & -r_2 \end{pmatrix} \sin\theta. \tag{A.6}$$

The eigenwaves $1^{\pm}$ and $2^{\pm}$ become decoupled and the defect modes combine only the localized components $1^{\pm}$. Thus, the defect mode can be defined using the 2×2 matrices U_{11} instead of the 4×4 matrix U, a fact which greatly simplifies the computations.

References

[1] Hodgkinson J J *et al* 2000 *Opt. Commun.* **184** 57
[2] Becchi M *et al* 2004 *Phys. Rev.* B **70** 033103
[3] Kopp V I and Genack A Z 2002 *Phys. Rev. Lett.* **89** 33901
[4] Kopp V I *et al* 2002 *Proc. SPIE* **4655** 141
[5] Wang F and Lakhtakia A 2003 *Opt. Commun.* **215** 79
[6] Schmidtke J and Stille W 2003 *Eur. Phys. J.* E **12** 553
[7] Oldano C 2003 *Phys. Rev. Lett.* **91** 259401
[8] Kopp V I and Genack A Z 2003 *Phys. Rev. Lett.* **91** 259402
[9] Lakhtakia A 2000 *Sensors Actuators* A **87** 78
Lakhtakia A 2000 Letter to the editor *Sensors Actuators* A **87** 78
[10] Oldano C *et al* 2003 *Phys. Rev.* E **67** 056624
[11] For additional bibliography on sonic crystals with twist defects, see Lakhtakia A 2003 *Sensors Actuators* A **104** 188
[12] Schmidtke J *et al* 2003 *Phys. Rev. Lett.* **90** 83902
[13] Ozaki M *et al* 2003 *Japan. J. Appl. Phys.* Part 2 **42** L472
[14] Song M H *et al* 2004 *Sci. Technol. Adv. Mater.* **5** 437
[15] Smith D R *et al* 1993 *J. Opt Soc. Am.* B **10** 314
[16] Kats E I 1970 *Zh. Eksp. Teor. Fiz.* **59** 1854
Kats E I 1971 *Sov. Phys.—JETP* **32** 1004
[17] Landau L *et al* 1984 *Electrodynamics of Continuous Media* (Oxford: Pergamon)
[18] Altman C and Sucky K 1991 *Reciprocity, Spatial Mapping and Time Reversal in Electromagnetics* (Dordrecht: Kluwer)
[19] Lindell I V 1994 *Electromagnetic Waves in Chiral and Bi-isotropic Media* (Boston, MA: Artech House)